Spatial Variations in Submolecular Vibronic Spectroscopy on a Thin Insulating Film

N. Ogawa, G. Mikaelian, and W. Ho*

Department of Physics and Astronomy and Department of Chemistry, University of California, Irvine, California 92697-4575, USA

(Received 23 January 2007; published 20 April 2007)

Scanning tunneling spectroscopy on single naphthalocyanine molecules adsorbed on an ultrathin aluminum oxide film exhibits electron-vibronic coupling that varies with the position of tunneling over the molecule. The spectra at different positions are composed of several series of equally spaced peaks, which are interpreted as progression of progressions of molecular vibrational modes. The spatial variations correlate with the molecular orbital structure, revealing spatially dependent electron-vibronic coupling and selective vibrational excitation.

DOI: 10.1103/PhysRevLett.98.166103 PACS numbers: 63.22.+m, 68.37.Ef, 73.40.Gk, 73.63.−b

Vibrational motion in molecular species and its coupling to the environment are of fundamental importance in molecular science and potential nanoscale device application. Vibrational excitation has been investigated with optical methods [1], in molecular junctions [2] down to the single molecule scale [3], and its dynamics has been resolved with femtosecond time resolution [4,5]. However, measurements with submolecular resolution would provide new understanding of the correlation of the molecular structure with vibrational coupling, spatial coherence, and energy redistribution within polyatomic molecules.

Vibrations of single molecules have been spatially resolved with the scanning tunneling microscope (STM) via inelastic electron tunneling spectroscopy (IETS) [6] and vibronic spectroscopy [7]. The selection rules for vibrational excitation in IETS are not the same as those of infrared absorption, Raman, or electron energy loss spectroscopies [8–10]. The observed vibrations are denoted as tunneling active modes [11]. In the case of vibronic spectroscopy, an electron is resonantly tunneled into a molecular orbital to form a vibronically excited anion. The vibronic states are strongly coupled to the electron and can be detected as peaks or shoulders in the dI/dV spectra [7,12]. For the detection of vibronic signals, thin insulating films have been utilized to reduce spectral broadening due to electronic interaction between the adsorbate and the metal substrate. In addition, the weak electronic coupling to the nanoenvironment leads to an extended lifetime for the transient state, enabling the detection of molecular fluorescence [13] and vibronic progressions [7,14] within the molecular electronic resonances.

Submolecular vibronic spectroscopy with the STM has been reported for several single molecules adsorbed on the ultrathin aluminum oxide film. The spacing of the peaks in the progression (i.e., vibrational energy) at different locations of a single copper phthalocyanine (CuPc) [7] or fullerene [15] remains the same. In addition, the overall shape of the spectra is similar, including the relative intensities of the peaks. Although the π-electron systems of organic molecules are delocalized, selective excitation and localization of molecular vibrations can be expected for larger molecules. Compared to phthalocyanine molecules, naphthalocyanine (NPc) has benzo rings attached to each isoindole subunit, providing an extended π-electron system that leads to similar but distinct optical, electrical, and catalytic properties, such as the redox potential.

The experiments were carried out with a homebuilt ultrahigh-vacuum STM at 11 K [16]. The double-barrier tunnel junction refers to the vacuum and the oxide barriers in the STM-tip/vacuum-gap/NPc-molecule/oxide/NiAl(110) structure [Figs. 1(a) and 1(b)]. The uniformly thin aluminum oxide film ($\approx$5 Å) was prepared by partial oxidation of the clean NiAl(110) surface [13,14]. The 2,3-naphthalocyanine molecules were thermally sublimated onto the oxidized surface at 11 K. An electrochemically etched Ag wire was used for the STM tip.

A typical conductance (dI/dV) spectrum of a NPc molecule is shown in Fig. 1(c), where the features at negative ($\sim-$ 1.4 V) and positive ($\sim$1.0 V) sample bias are attributed to the highest occupied (HO) and lowest unoccupied (LU) molecular orbitals (MO), respectively. For the lowest unoccupied molecular orbital (LUMO), vibronic features are resolved. Because of the inherent inhomogeneity of the oxide film grown on NiAl [17], the molecules experience different local environments at each adsorption site, leading to a distribution of onset energy for the molecular electronic states. The onset of the highest occupied molecular orbital (HOMO) state appears below -1.0 V, whereas the onset for the LUMO state is between 0.15 to 1.0 V.

STM topographic images were taken at biases corresponding to the HOMO state, the LUMO state, and in the conductance gap [insets of Fig. 1(c)], revealing the orbital structures of NPc. On the HOMO state, fine structures inside the molecule and four pairs of larger protrusions are resolved. The LUMO state has broad density of states centered on the molecule, and the fine structures are smeared out due probably to the presence of states that are separated by small energies [18]. These states have similar orbital structure and are orthogonal to each other [19]. For the LUMO state, the appearance of "nodes" in the image is in clear contrast to CuPc [7]. In the conduc-

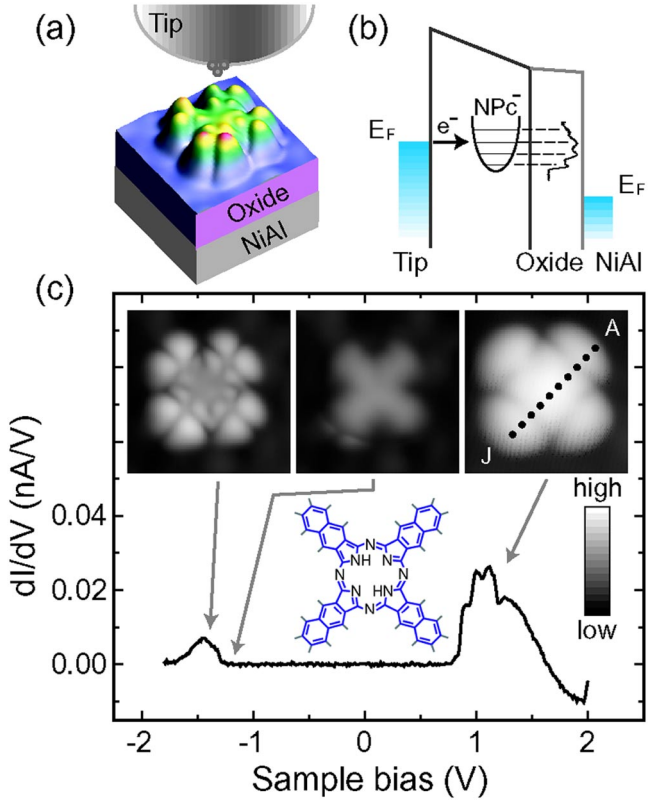

FIG. 1 (color online). (a) A double-barrier tunnel junction. (b) Schematic representation for the resonant electron tunneling into the anion vibronic states of a single molecule (for positive sample bias). (c) dI/dV spectrum of a naphthalocyanine (NPc) molecule adsorbed on the oxide surface grown on NiAl(110). The tunneling gap was set with 2.0 V sample bias and 100 pA tunneling current. The bias modulation was 7 mV (rms) at 327 Hz. Insets show a schematic of NPc-molecule and constant-current (17 pA) STM images (4 nm × 4 nm) with sample bias of −1.35 V (left), −1.2 V (center), and 1.2 V (right). Images are not filtered. Dotted line within the right-hand image represents the positions of d^2I/dV^2 mapping shown in Fig. 2.

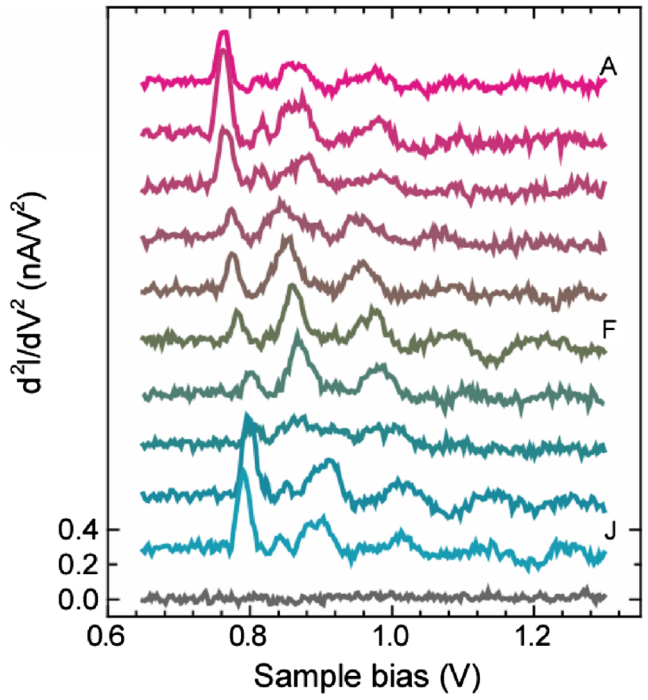

FIG. 2 (color online). d^2I/dV^2 spectroscopic mapping taken across a NPc molecule at positions equally spaced from point A to J, as shown in the inset of Fig. 1(c). The bottom curve represents the background signal over the oxide in the vicinity of the molecule. The set point for the tunneling gap was 1.3 V and 60 pA. The spectra are offset for clarity.

tance gap, the image reflects the overall geometric structure of the molecule and its interaction with the substrate.

The vibronic progressions in the LUMO appear as peaks in the d^2I/dV^2 spectra. A mapping across a NPc molecule is shown in Fig. 2 for a series of points above the molecule. On the lobes, near spectra A and J, the first peak with high intensity is followed by a small peak and several broad features. Around the center (F) of the molecule, the first peak has relatively low intensity, and a broad second peak appears at different energy compared to nearby peaks on the lobes. The peak onsets show slight shifts across the molecule; however, the overall spectral features are spatially symmetric about the center (F). For molecules with different adsorption geometries, spectra taken over the center of the molecule have similar structures, and spectra on the lobes usually show more features than those over the center. Although the vibronic states should correspond to peaks in the dI/dV spectra, peaks in d^2I/dV^2, detecting the inflection points of the steplike features in the dI/dV spectra, contain the same information on the energy spacing between vibronic peaks, and similar information for the peak width.

Each d^2I/dV^2 spectrum is fit to a series of Gaussian peaks by taking the width of the first peak as the experimental linewidth [20]. The spectra are composed of multiple sequences of equally spaced peaks. By extracting the peak energies from several spectra across the molecule, and fixing relative peak positions, least-square fitting is performed for each spectrum with 13 Gaussian profiles. The results for spectra F (over the center of the molecule) and J (on the lobe) are shown in Figs. 3(a) and 3(b), respectively. All spectra can be well expressed with 4 progressions of vibronic states as shown in the figure.

Two sequences of vibronic progressions with the same spacing, displaced from each other with the energy of another vibrational mode, have been observed for single C_{60} [15] and Zn-etioporphyrin [21] adsorbed on thin aluminum oxide film on NiAl(110). These spectral features are attributed to ''progression of progressions,'' where each level of the first progression is the starting point for the other progressions [20]. In addition, vibronic features corresponding to several vibrational modes were observed for

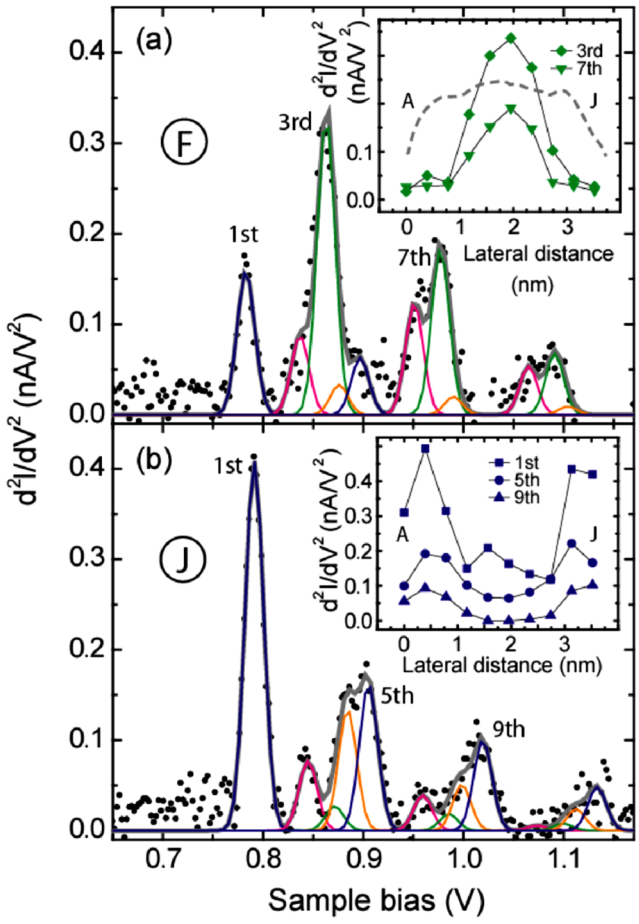

FIG. 3 (color online). Curve fittings of the d^2I/dV^2 spectra (a) F (in the center) and (b) J (on the lower left lobe) with a series of equally- spaced Gaussian functions. The resolved peaks are grouped into 4 progressions. The first progression is composed of the first, fifth, ninth, and thirteenth peaks. Second progression: second, sixth, and tenth peaks. Third progression: third, seventh, and eleventh peaks. Fourth progression: fourth, eighth, and twelfth peaks (see text for detail). These progressions are indicated by the blue, magenta, green, and orange lines, respectively (color online). The summation of the fitted peaks is the curve following most closely the data points (gray line in color online). Insets show the spatial distribution of the peak intensity for the first (first, fifth, and ninth peaks, lower panel) and third (third and seventh peaks, upper panel) progressions. The topographic trace of the molecule at the set point for mapping is also shown in the upper inset (dashed curve, ~0.5 nm in height).

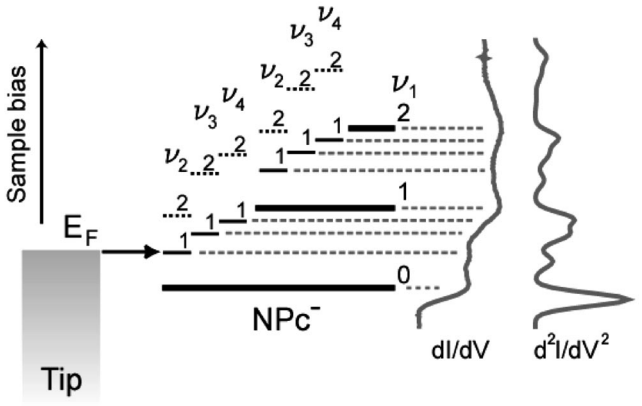

FIG. 4. Schematic representation of the progression of progressions for a NPc molecule. The principal vibronic states (υ_1) are denoted by thick lines, from which the energies for the other vibrational modes (υ_2, υ_3, υ_4) are measured. The second excited states for υ_2, υ_3, and υ_4 vibrations are not resolved in the experiment. With increasing sample bias, the Fermi level of the tip aligns with each vibronic substate one after the other, and the tunneling probability increases. The corresponding spectral features in dI/dV and d^2I/dV^2 spectra are indicated on the right.

$Ag(C_{60})_3$ charge transfer complex in the C_{60} monolayer on the aluminum oxide film [22]. Since the same peak spacing is observed for NPc molecules with different adsorption geometries distinguished by different LUMO onset voltage, and the peaks exhibit distinct spatial dependences, the 4 progressions are progression of progressions of 4 different molecular vibrational modes, as schematically shown in Fig. 4. The spatial distribution of each progression cannot be explained by the existence of nearly degenerated LUMO orbitals. Taking into account the contributions to the linewidth from the thermal and modulation broadenings in the vibronic spectra, an estimate for the lifetime of the anionic state is $\approx$ 100 fs, which is 4 orders of magnitude shorter than the time interval between successive tunneling events. The origin of the observed vibronic progressions as due to multiple excitations can thus be ruled out. The molecule is in its ground state when an electron tunnels from the tip.

The 4 progressions have common peak spacing of 114 meV (υ_1), and relative energy shifts of 54 (υ_2), 80 (υ_3), and 93 meV (υ_4) for second, third, and fourth progressions, respectively, as measured from the onset energy of the first progression. For NPc molecules with different LUMO onsets, peak spacing of about 115 meV (υ_1), and relative shifts close to 50 (υ_2) and 80 meV (υ_3), have been commonly observed. The insets of Fig. 3 show the spatial variation of the peak intensity across the molecule for different progressions. The first progression (υ_1, composed of first, fifth, ninth, and thirteenth peaks, bottom inset) has high intensity on the lobes, whereas the third progression (υ_3, third and seventh peaks, top inset) is observed over the center of the molecule. These results demonstrate the spatial dependence of the coupling of electrons to different vibrational modes.

The similarity in the spatial distribution of the peak intensity in each progression, such as the third and seventh peaks, would be consistent with assigning them to the same vibrational mode. The topographic trace of the molecule at the set point for spectroscopy is also shown in Fig. 3(a), top inset. The change in the tip height is small from the center to the lobe of the molecule. Therefore, the observed spatial

variations do not stem from the changes in the tip height. The spatial distributions of the second and fourth progressions (not shown) have similar trends as the third and first progressions, respectively, although the overall intensity is weaker. From the analysis of the spatial distribution of the peak intensities, the voltage drop in the oxide film (5%–20% of the total bias voltage [7]), and comparison to IR and Raman spectra of NPc in the solid matrix [23,24], the υ_1 vibration can be assigned to the naphthalene breathing (111 meV), υ_2 to the skeletal distortion of isoindole (60 meV), υ_3 to the Pc breathing or pyrrole skeletal distortion (84 meV), and υ_4 to the naphthalene skeletal distortion (89 meV).

In the resonant tunneling mechanism, an electron from the tip tunnels into the LUMO orbital to form a transiently charged anionic state. Although π-electron systems are delocalized, those bonds that lie within the density of states of the LUMO at the position of tunneling will be effectively excited. The subsequent motions of these bonds, due to differences in neutral and ionic configurations, the strength of the electron-vibrational coupling, and the lifetime of the anionic state define the prominent vibronic progressions in the spectra. This is in clear contrast with the nonlocal optical excitation, where the spectral shape is governed by the Franck-Condon integral of all the allowed states at the excitation energy. Furthermore, in the original notion of progression of progressions, the third progression should have the energy relative to the second progression, which differs from our observation. This difference may arise from the above mentioned ''local excitation,'' which excites local vibrations with the energy relative to the anion levels.

The observed vibrational modes are well localized in different parts of the molecule. Compared to the case of CuPc, where only one vibronic progression is identified within the molecule [7], NPc is about 5 Å larger, and has nodes that separate the central part of the molecule from the lobes in STM images. As shown in the inset of Fig. 3(a), excitation of the υ_3 vibronic mode is confined within the nodes of the molecular orbital. For the υ_1 mode [inset of Fig. 3(b)], although the excitation is localized on the outermost benzene rings, the observed vibration involves the naphthalene structure and extends beyond the nodes [Fig. 1(c)]. These results suggest that the nodal structure affects the coherence of the vibrational excitation, and vibrational modes can be selectively excited by positioning the STM tip relative to the nodes of orbitals.

This work was supported by the Air Force Office of Scientific Research, Grant No. FA9550-04-1-0181. We thank M. Persson, M. Janson, M. Lackinger, X. Chen, S. W. Wu, and C. Chen for insightful discussions. N. O. received support from JSPS.

*Electronic address: wilsonho@uci.edu

[1] *Modern Molecular Photochemistry*, edited by N. J. Turro (Benjamin/Cummings, Menlo Park, CA, 1978).
[2] *Molecular Nanoelectronics*, edited by M. A. Reed and T. Lee (American Scientific, Stevenson Ranch, CA, 2003).
[3] See, for example, A. B. Myers *et al.*, J. Phys. Chem. **98**, 10 377 (1994), and references therein.
[4] A. H. Zewail, J. Phys. Chem. A **104**, 5660 (2000).
[5] *Ultrafast Infrared And Raman Spectroscopy*, edited by M. D. Fayer (Marcel Dekker, New York, 2001).
[6] B. C. Stipe, M. A. Rezaei, and W. Ho, Science **280**, 1732 (1998).
[7] X. H. Qiu, G. V. Nazin, and W. Ho, Phys. Rev. Lett. **92**, 206102 (2004).
[8] P. Sautet and M.-L. Bocquet, Phys. Rev. B **53**, 4910 (1996).
[9] N. Lorente and M. Persson, Phys. Rev. Lett. **85**, 2997 (2000).
[10] N. Lorente *et al.*, Phys. Rev. Lett. **86**, 2593 (2001).
[11] W. Ho, J. Chem. Phys. **117**, 11 033 (2002).
[12] M. Galperin, A. Nitzan, and M. A. Ratner, Phys. Rev. B **73**, 045314 (2006), and references therein.
[13] X. H. Qiu, G. V. Nazin, and W. Ho, Science **299**, 542 (2003).
[14] S. W. Wu *et al.*, Phys. Rev. Lett. **93**, 236802 (2004).
[15] N. A. Pradhan, N. Liu, and W. Ho, J. Phys. Chem. B **109**, 8513 (2005).
[16] B. C. Stipe, M. A. Rezaei, and W. Ho, Rev. Sci. Instrum. **70**, 137 (1999).
[17] G. Kresse *et al.*, Science **308**, 1440 (2005).
[18] X. Zhang, Y. Zhang, and J. Jiang, J. Mol. Struct., Theocem **673**, 103 (2004).
[19] M. Lackinger *et al.*, J. Phys. Chem. B **108**, 2279 (2004).
[20] *Spectra of Polyatomic Molecules*, edited by G. Herzberg (Van Nostrand & Reinhold, New York, 1966).
[21] H. J. Lee, J. H. Lee, and W. Ho, Chem. Phys. Chem. **6**, 971 (2005).
[22] G. V. Nazin, X. H. Qiu, and W. Ho, J. Chem. Phys. **122**, 181105 (2005).
[23] S. M. Arabei *et al.*, Chem. Phys. **311**, 307 (2005).
[24] I. Gobernado-Mitre and R. Aroca, Chem. Mater. **7**, 118 (1995).